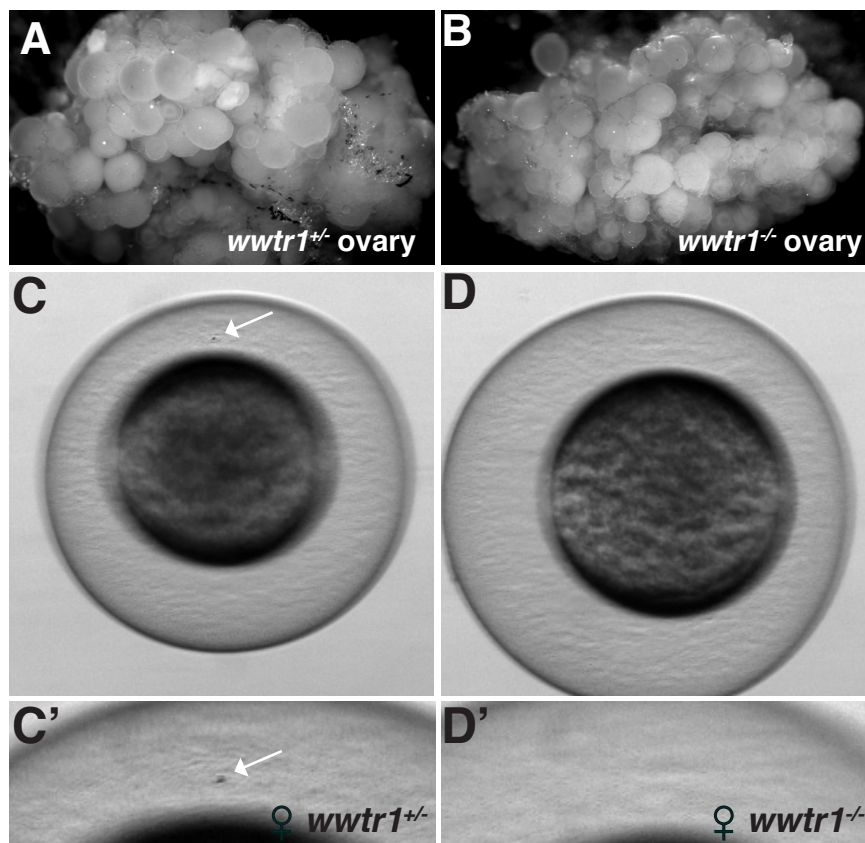


**Fig. S1. Characterization of the *wwtr1<sup>fu55</sup>* allele**

(A) TALEN target sequence within the *wwtr1* exon1. TAL repeats are color-coded. A BspHI site in the spacer region was used for genotyping. (B, C) The *fu55* allele has one inserted and eight deleted base pairs (B) leading to a premature STOP codon after 29AA (C). (D, E) *wwtr1<sup>-/-</sup>* adult fish (E) are indistinguishable from *wwtr1<sup>+/-</sup>* adult fish (D). (F-K) While, embryos from three independent crosses between *wwtr1<sup>mw49/+</sup>* heterozygous females and WT males developed normally (F-H), eggs from three independent crosses between *wwtr1<sup>mw49/fu55</sup>* trans-heterozygous females and WT males were all unfertilized (I-K). Scale bars: 1 cm in D-E



**Fig. S2 Ovaries and micropyle in *wwtr1*<sup>-/-</sup> mutant**

(A-B) Whole ovaries from *wwtr1*<sup>+/-</sup> (A, n=2 ovaries) and *wwtr1*<sup>-/-</sup> females (B, n=2 ovaries) are indistinguishable. (C-D') The micropyle is visible at the surface of the chorion in activated eggs from *wwtr1*<sup>+/-</sup> (C, C' white arrow, N=3, n=20) but not from *wwtr1*<sup>-/-</sup> (D, D' N=3, n=20) females.

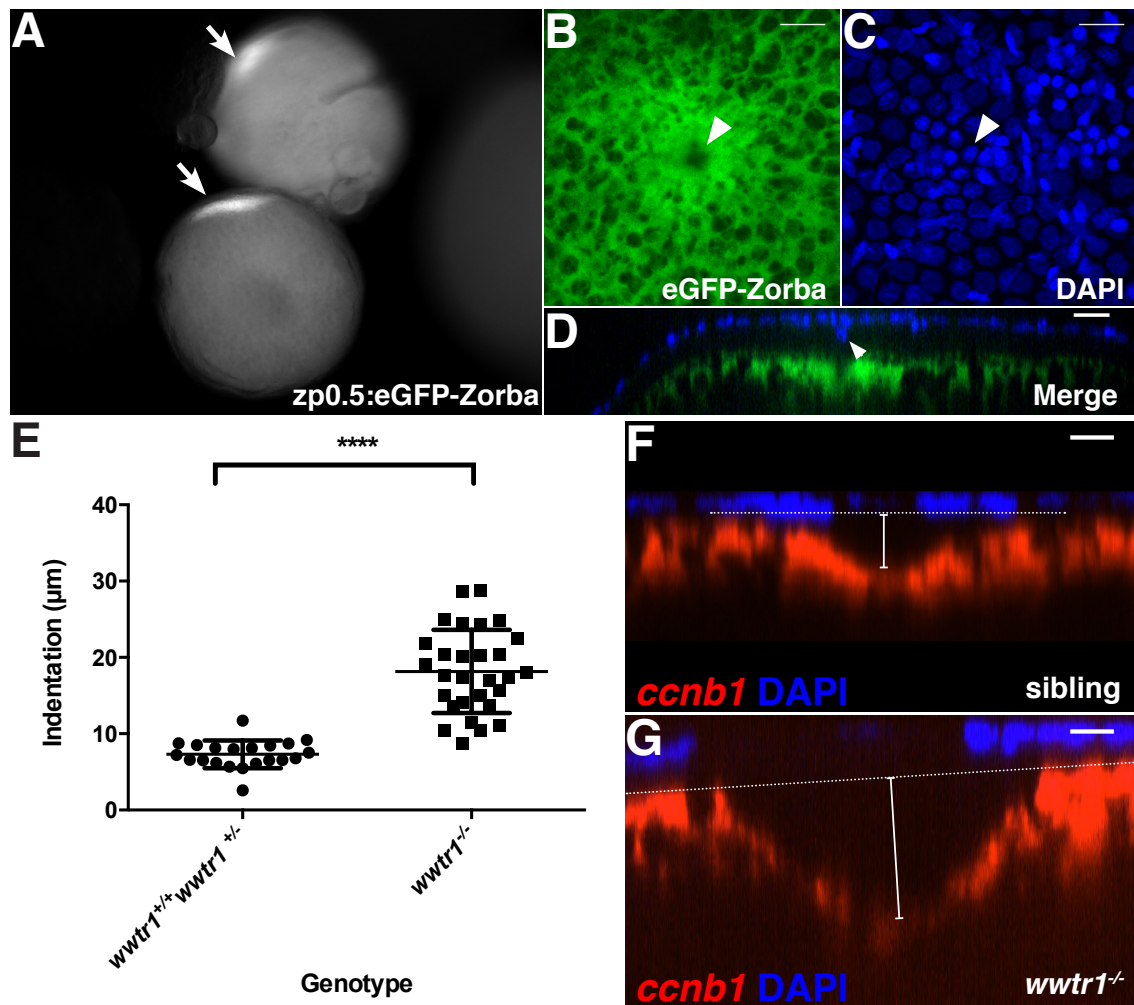


**Fig. S3. Oocytes from F0 females expressing eGFP-Zorba and quantification of the indentation of the animal pole oocyte surface**

(A) Overview image of two stage III oocytes showing the product of the *eGFP-zorba* transgene restricted to a particular domain at the periphery of the oocyte (white arrow). (B) A small indentation (white arrowhead) is present in the center of the eGFP-Zorba positive region. (C) Nuclei are organized in a concentric pattern around the MC nucleus (white arrowhead) coinciding with the indentation observed in (B). (D) Orthogonal view of the confocal stack, shown as maximum intensity projection in B and C, showing the animal pole localization and enrichment of the eGFP-Zorba, and the centrally overlying MC (white arrowhead). (E) Quantification of the indentation of the animal pole oocyte surface in *wwtr1*<sup>-/-</sup> (51% of the mutants showed an indentation N=4 - n=54), and *wwtr1*<sup>+/+</sup> and *wwtr1*<sup>+/-</sup> (100% N=4 - n=42) follicles. Data are represented as mean ± S.E.M - two-tailed *t*-test *P*<0.0001. (F-G) Orthogonal views of confocal stacks of whole-mount follicles from *wwtr1*<sup>-/-</sup> females (G) or sibling (F) stained by WISH to visualize *ccnb1* mRNA and DAPI. The vertical bars in F and G indicate how the depth of the indentation was measured.

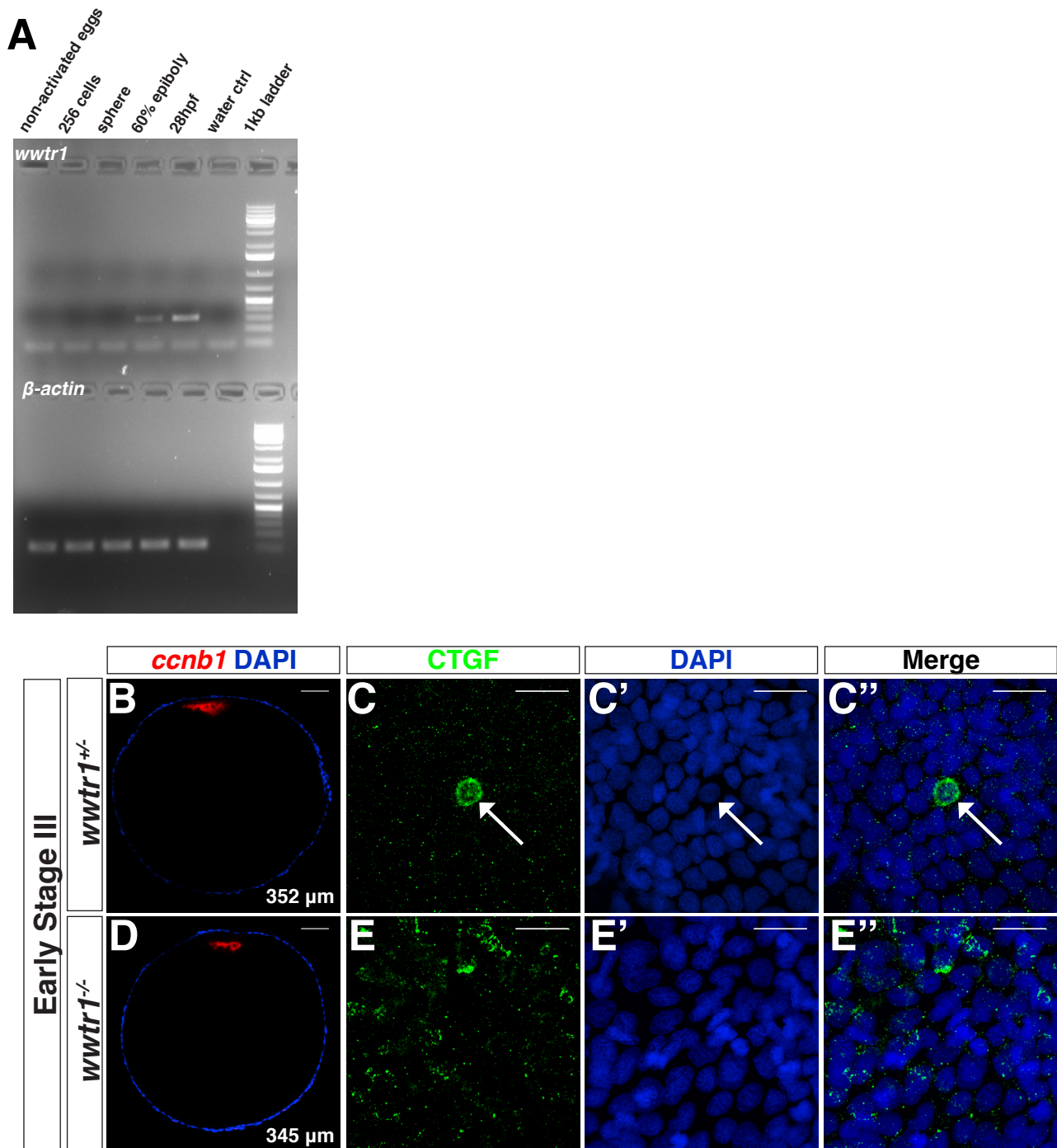


**Fig. S4. *wwtr1* expression during early zebrafish embryogenesis and CTGF immunostaining**

(A) Reverse-transcription experiment to detect *wwtr1* mRNA expression (upper row) in non-activated eggs (lane1) or in embryos before (256 cell stage, lane 2) or after (lane 3 to 5) the zygotic genome activation. Lane 6 is a negative control without mRNA. The lower part of the gel shows the amplification of  $\beta$ -actin mRNA from the same total RNA.  $\beta$ -actin is known to be expressed maternally and is used as a positive control. Ladder used in lane 7 is 1kb plus.

(B-E'') Whole mount immunostaining of *wwtr1*<sup>+/-</sup> and *wwtr1*<sup>-/-</sup> early stage III follicles with an antibody against the bona fide YAP1/TAZ target CTGF. B and D show overview images to determine the oocyte size (as indicated in the lower right corner) and thus their stage. Follicles were counterstained with DAPI to label the FC nuclei. The white arrows point to the MC in (C, C', C'') at the animal pole while no such staining was observed in *wwtr1*<sup>-/-</sup> follicles (E, E', E''). Scale bar: 50  $\mu$ m in B, D and 10  $\mu$ m in C,E.

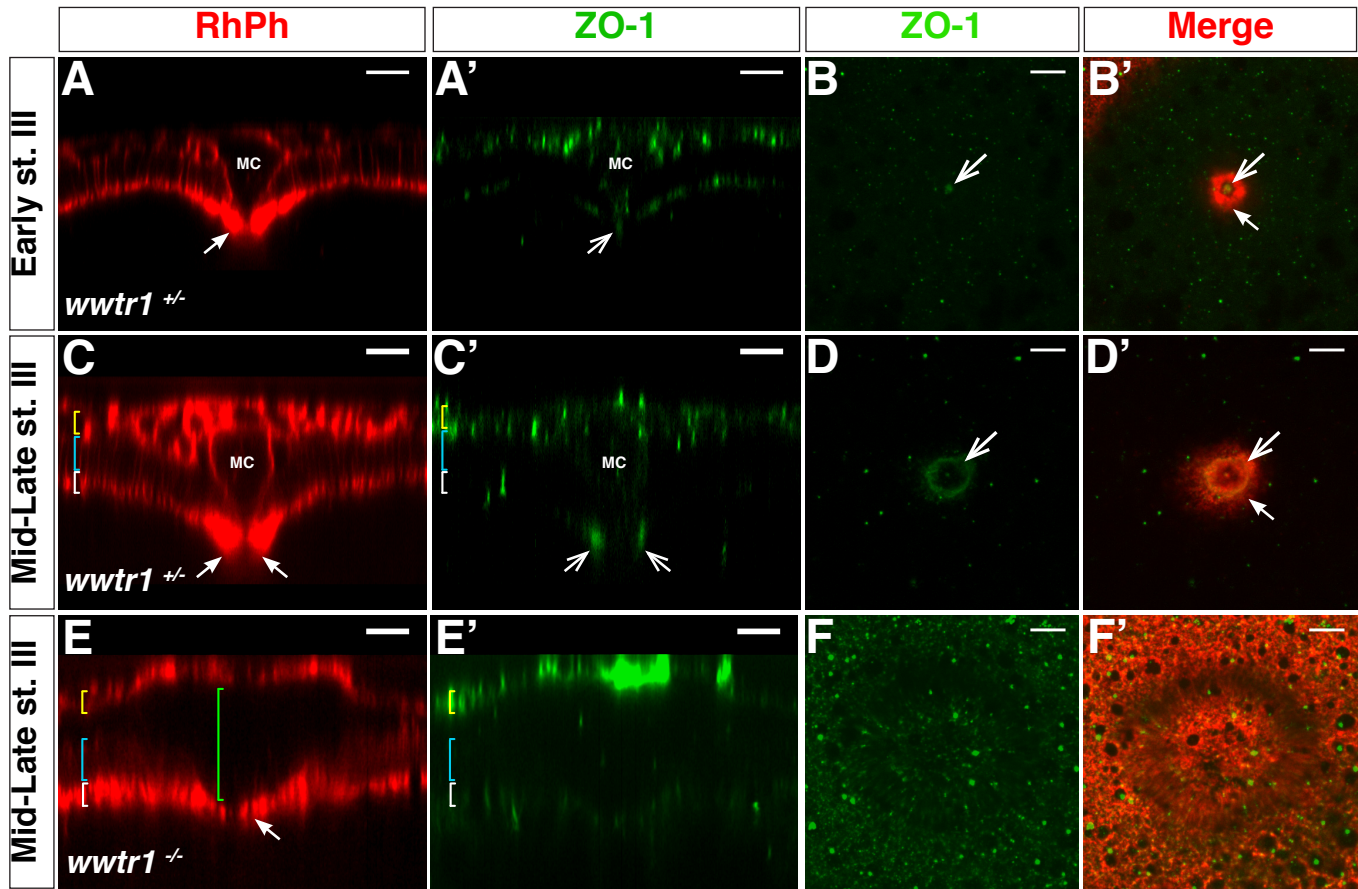


**Fig. S5. The MC contacts the oocyte surface via ZO-1 containing junctions**

(A-F') Whole-mount *wwtr1*<sup>+/+</sup> (A-D') and *wwtr1*<sup>-/-</sup> (E-F') follicles stained with Rhodamine Phalloidin to label F-actin, and an anti-ZO1 antibody to label tight junctions (N=2, n=10). (A, C, E) are orthogonal views of the oocyte animal pole with the FC layer on top (yellow bracket). (B, D, F) are confocal projections of the oocyte animal pole (stack size 4 μm). Solid and simple arrows point to Actin and ZO-1 localization at the contact point, respectively. Animal views of the follicle show the indentation at the animal pole of the *wwtr1*<sup>-/-</sup> oocyte (F, F'). White, blue and yellow brackets mark the oocyte cortex, the layer of microvilli and the FC layer, respectively. MC: Micropylar cell. Scale bar: 10 μm.

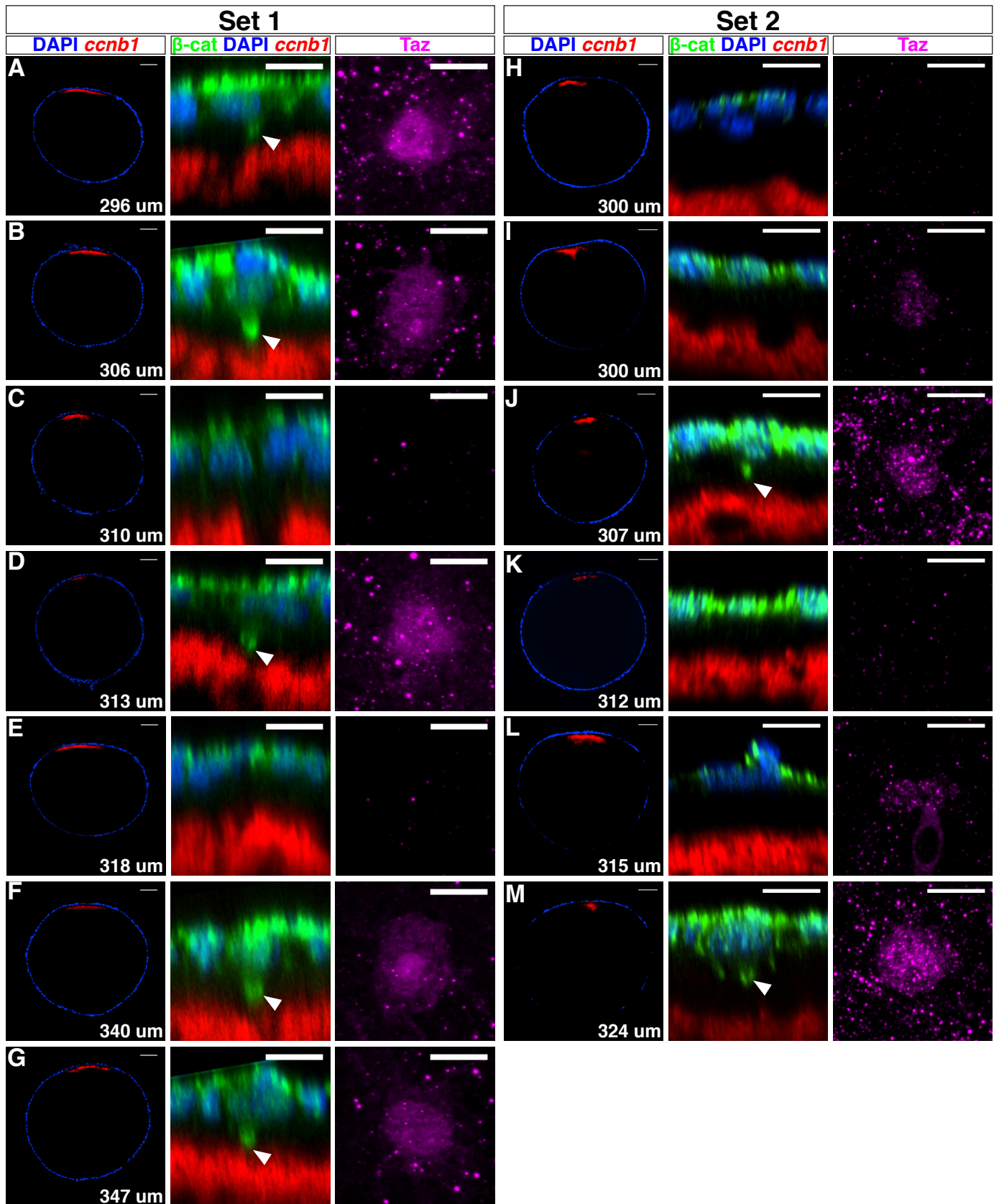


**Fig. S6. Taz enrichment occurs before morphological changes of the MC**

(A-M) show two sets of immunostainings on whole-mount WT follicles with Taz and  $\beta$ -catenin antibodies. DAPI counterstaining and *ccnb1* WISH have been performed to label the FC nuclei and localize the oocyte animal pole, respectively. In each set, all left panels show overview images to determine the oocyte size (as indicated in the lower right corner) and thus their stage. The middle panels are orthogonal views of confocal stacks at the level of the MC precursor. The white arrowhead points to the  $\beta$ -catenin-enriched apical tip of the MC precursor. The right panels are maximum intensity projection of the corresponding confocal stack showing Taz staining. Follicles C, E, H and K have no Taz staining in the MC precursor yet. Scale bar: 10  $\mu$ m, overview images 50  $\mu$ m.

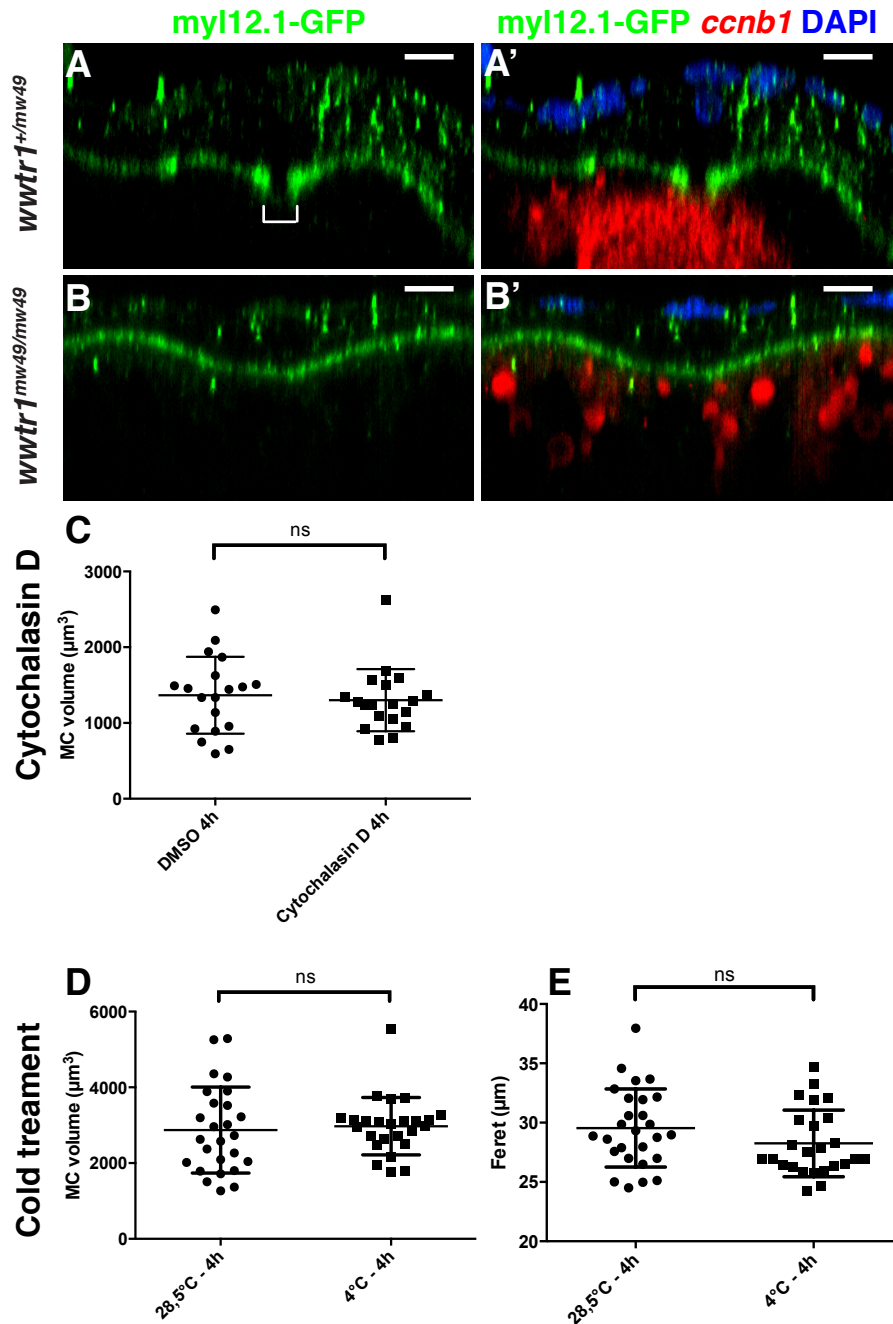


**Fig. S7. The gap in the oocyte non-muscle myosin cortex is MC-dependent and consequence of actin and stable microtubule destabilization on the MC**

(A-B) Orthogonal views of confocal stacks of *actb1:myl12.1-eGFP* transgenic follicles, either *wwtr1<sup>mw49/+</sup>* (A,A') or *wwtr1<sup>mw49/mw49</sup>* (B,B'). These were stained by WISH with *ccnb1* to localize the animal pole and with DAPI to label the FC nuclei. A zone with strongly reduced Myl12.1-GFP is visible in *wwtr1<sup>mw49/+</sup>* (white bracket in A, A') but not in *wwtr1<sup>mw49/mw49</sup>* follicles (B, B'). (C-E) shows the quantification of the volumes (C-D) or Feret (E) of the MC after segmentation either after cytochalasin D treatment (C) to destabilize actin filament or after cold treatment (D-E) to destabilize stable microtubules. Data are represented as mean  $\pm$  S.E.M. P values were calculated using unpaired, two-tailed *t*-test and revealed non significant differences in all 3 cases.  $P=0,67$  (C),  $P=0,70$  (D) and  $P=0,14$  (E).

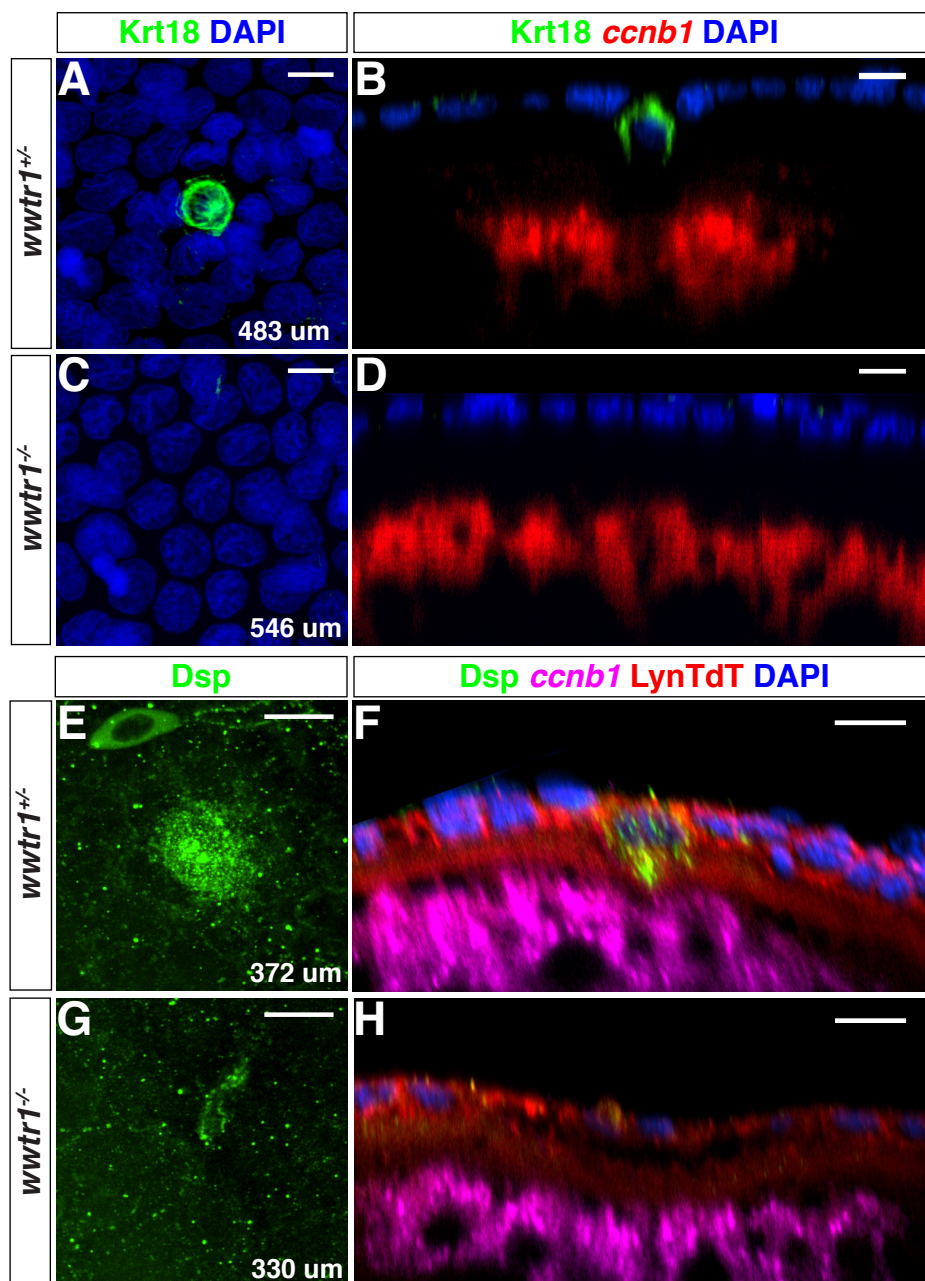


**Fig. S8. Keratin and Desmoplakin protein are absent from the FCL in *wwtr1*<sup>-/-</sup> mutants.**

(A-H) Confocal stacks of whole-mount immunofluorescence with an antibody against the intermediate filament protein Krt18 (A-D), or Dsp (E-H) shown as maximum intensity projection (A, C, E, G) or orthogonal views (B, D, F, H). DAPI counterstaining and *ccnb1* WISH have been performed to label the FC nuclei and localize the oocyte animal pole, respectively. Oocytes in (E-H) carry the *actb2:lyn-TdT* transgene. Scale bar: 10 μm.

**Table S1 Fertilization rates**

	inX <i>wwtr</i> <sup><i>fu55/fu55</i></sup>		inX <i>wwtr</i> <sup><i>+/fu55</i></sup>	
	total	fertilized	total	fertilized
cross1	314	14	235	200
cross2	342	0	390	335
cross3	166	0	291	273
cross4	31	0	516	450
cross5	310	0	246	218
total	1163	14	1678	1476
percentage		<b>1</b>		<b>88</b>

	inX <i>wwtr</i> <sup><i>mw49/mw49</i></sup>		inX <i>wwtr</i> <sup><i>+/mw49</i></sup>	
	total	fertilized	total	fertilized
cross1	164	0	165	161
percentage		<b>0</b>		<b>98</b>

**Table S1.** Comparison of fertilization rates in *wwtr*<sup>*fu55/fu55*</sup> versus *wwtr*<sup>*+/fu55*</sup> incrosses (top, 5 independent crosses) and *wwtr*<sup>*mw49/mw49*</sup> versus *wwtr*<sup>*+/mw49*</sup> incrosses (bottom, 1 cross).

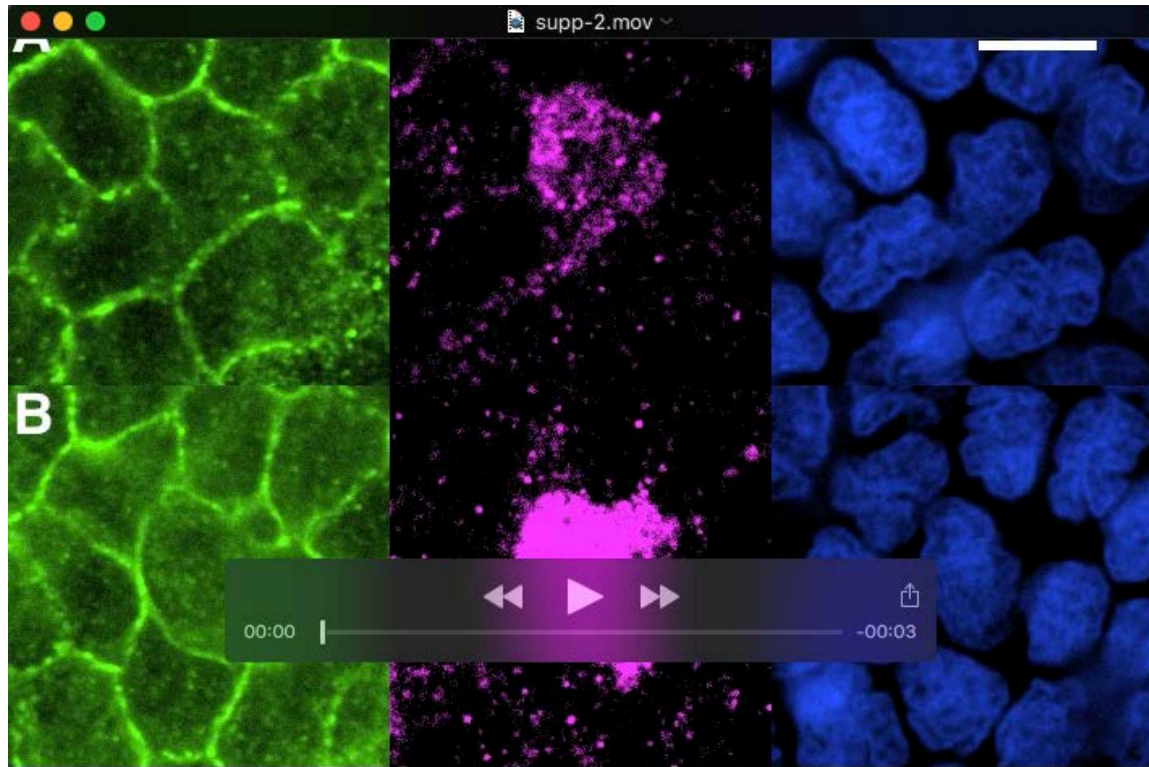
**Table S2 Fertilization rates upon IVF without chorion**

	<i>wwtr1</i> <sup>+/-</sup> mutant female		<i>wwtr1</i> <sup>-/-</sup> mutant female	
	Number	%	Number	%
Collected Eggs	685	100.00	649	100.00
Fertilized Eggs	162	23.65	155	23.88
- Blastula	69	10.07	108	16.64
- Partial cleavage	93	13.58	47	7.24
Embryos 1 dpf	4	0.58	26	4.01
- Abnormal	3	0.44	13	2.00
- Normal	1	0.15	13	2.00

**Table S2.** Comparison of fertilization rates and further development of eggs from *wwtr1*<sup>+/-</sup> and *wwtr1*<sup>-/-</sup> females, fertilized *in vitro* after enzymatic digestion of the chorion. Approximately 24% of the eggs were fertilized in each case. From these 24%, 4% eggs from the *wwtr1*<sup>-/-</sup> females underwent development until 1dpf against less than 1% eggs from the *wwtr1*<sup>+/-</sup> females.

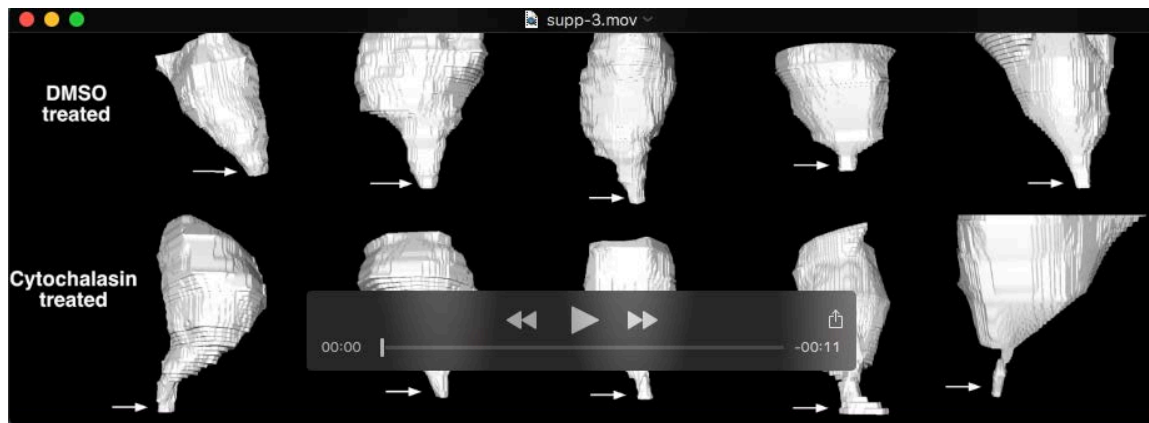
**Table S3 List of primers**

<b>Primer name</b>	<b>Primer sequence (5' to 3')</b>	<b>Procedure</b>
<i>wwtr1 -tal1-e1-fow</i>	ACACTTTTCAACTCGGCTGA	TALEN screening
<i>wwtr1 -tal1-e1-rev</i>	AAAGTACTTCTGGCCGTTGG	TALEN screening
<i>bactin2_BamHI_Fwd</i>	ATGCCGGATCCAATTCCAGTTTGAAGAAACTTTTCAA	Tg( <i>bactin2:lynTdT</i> )
<i>bactin2_NotI_Rev</i>	GGCATGCGGCCGCGGCTGAACTGTAAAAGAAAGGG	Tg( <i>bactin2:lynTdT</i> )
<i>lynTdT_BamHI_Fwd</i>	TGCATGGATCCATGGGCTGCATCAAGAGCA	Tg( <i>bactin2:lynTdT</i> )
<i>lynTdT_XhoI_Rev</i>	AGAGGCTCGAGTTACTTGTACAGCTCGTCCAT	Tg( <i>bactin2:lynTdT</i> )
<i>-0.5zp3b_BglII_Fwd</i>	GATCCAGATCTAAAATCCCCATGACATGCTGC	Tg( <i>-0.5zp3b:eGFP-zorba</i> )
<i>-0.5zp3b_NotI_Rev</i>	GGATCGCGGCCGCATTGCCTGCTGACTAATTAAACC	Tg( <i>-0.5zp3b:eGFP-zorba</i> )
<i>zorba_EcoRI_Fwd</i>	AAGACGAATTCGATGGCGTTTTTCTCTGAGAGAA	Tg( <i>-0.5zp3b:eGFP-zorba</i> )
<i>zorba_XhoI_Rev</i>	AGAGGCTCGAGTCAGTTGGCGTCCCGCTT	Tg( <i>-0.5zp3b:eGFP-zorba</i> )
<i>wwtr1_fwd</i>	CGCAGTCTTTCTTCCAGGAG	RT-PCR
<i>wwtr1_rev</i>	TGCCATGTGGTGATCTTCTC	RT-PCR
<i>bactin_fwd</i> (+ve control)	CGAGCTGTCTTCCCATCCA	RT-PCR
<i>bactin_rev</i> (+ve control)	TCACCAACGTAGCTGTCTTTCTG	RT-PCR



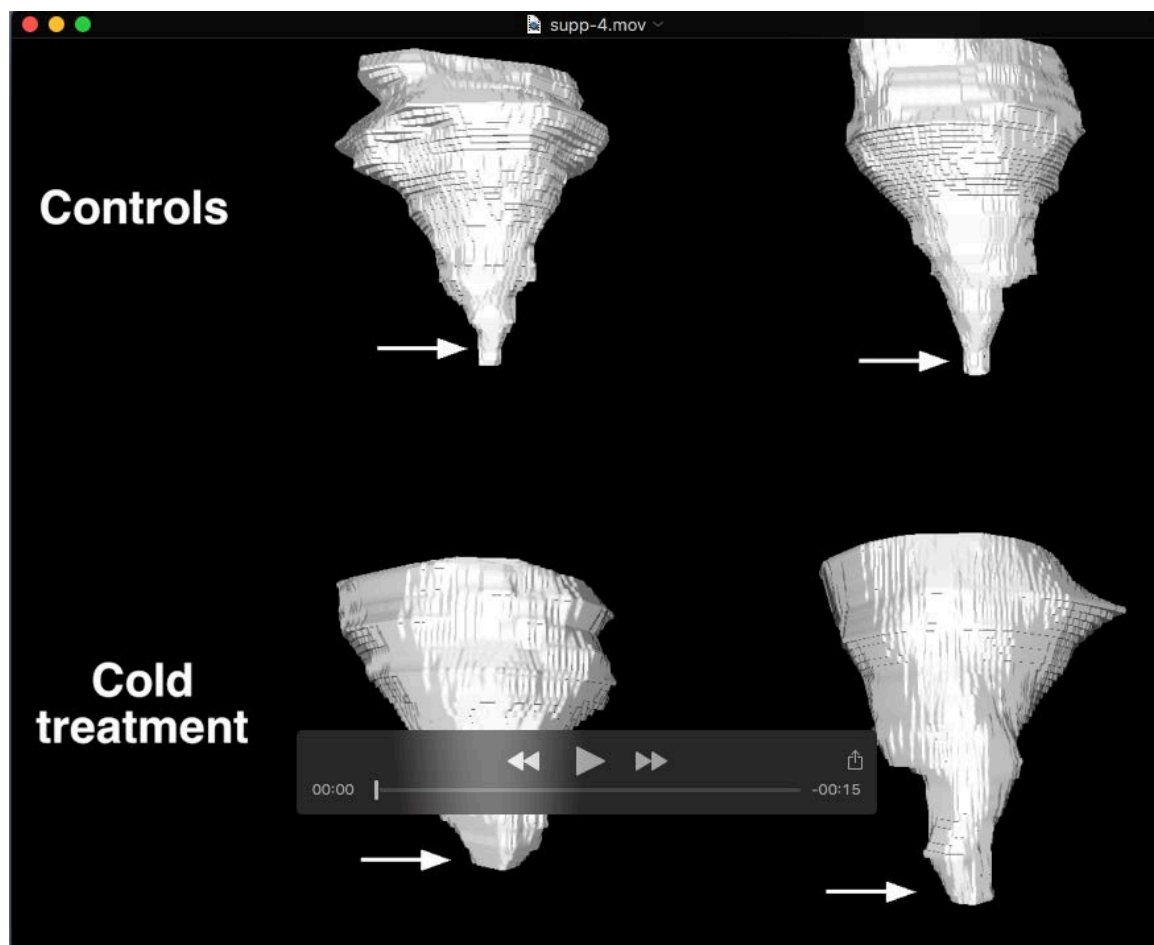
**Movie S1 Taz is enriched in the MC precursor before  $\beta$ -catenin apical enrichment and morphological changes of the cell**

(A-B) Animated confocal stacks of *wwtr1*<sup>+/+</sup> whole-mount follicles at the stage II (A, also shown in Fig. 5L-O) and early stage III (B, also shown in Fig. 5P-S) of oogenesis stained with Taz (magenta) and  $\beta$ -catenin (green) antibodies, and DAPI (blue). When Taz starts to be enriched (A, upper panel), the MC precursor is indistinguishable from neighbouring FCs in terms of shape, nuclear morphology and  $\beta$ -catenin localization. Once Taz levels increase in the MC precursor (B, lower panel),  $\beta$ -catenin is enriched at the contact point between the microvilli and the MC precursor (solid white arrow, in B) with still no obvious changes in the cell shape and nuclear morphology. The microvilli appear as densely-organized,  $\beta$ -catenin-positive spots in A and B. Scale Bar: 10  $\mu$ m.



### Movie S2 Consequence of Cytochalasin D treatment on the MC morphology

Movie S2 shows the 3D morphology of the MC at the mid-stage III of oogenesis upon DMSO and Cytochalasin D treatment. DMSO treated MCs (upper row) showed typical mushroom-shaped morphology with a shorter MC process (white solid arrow) while the Cytochalasin D treated MCs (lower row) showed an elongated MC process (white solid arrow)



### Movie S3 Consequence of cold treatment on the MC morphology

Movie S3 shows the 3D morphology of the MC at late stage III/early stage IV of oogenesis upon cold treatment. At 28.5°C, the MC process is longer and narrower (upper row, white solid arrow) while at 4°C it appears blunt and wider (lower row, white solid arrow).